Prediction of the thermo-energetic behaviour of an electrohydraulic compact drive

peer reviewed

Dipl.-Ing. Sebastian Michel

Institute of Fluid Power (IFD), Technische Universität Dresden, Helmholtzstrasse 7a, 01069 Dresden, E-mail: michel@ifd.mw.tu-dresden.de

Professor Dr.-Ing. Jürgen Weber

Institute of Fluid Power (IFD), Technische Universität Dresden, Helmholtzstrasse 7a, 01069 Dresden, E-mail: mailbox@ifd.mw.tu-dresden.de

Abstract

Due to good energy-efficiency of electrohydraulic compact drives a cooling aggregate often is not installed. The operating temperature is governed by the complex interaction between dissipative heat input and passive heat output. This paper targets the simulation of the thermo-energetic behaviour of an electrohydraulic compact drive by means of a lumped parameter model in order to predict the operating temperature. The developed thermo-hydraulic model is validated against measurements utilising thermocouples and a thermographic camera to capture temperatures. The results show, that the presented methodology enables a satisfying accurate prediction of the thermo-energetic behaviour of electrohydraulic compact drives. A further analysis of simulation results is given, highlighting the power losses and heat rejection capabilities of different components. Finally, measures for the improvement of the heat rejection capabilities are studied.

KEYWORDS: Electrohydraulic compact drive, EHA, thermo-energetic simulation, heat transfer processes

1. Introduction

Electrohydraulic compact drives are an interesting alternative to conventional hydraulic or electromechanical drives. Owing to the good efficiency a key property of electrohydraulic compact drives is the possibility to design the actuator without a cooling aggregate. The dissipated energy is discharged via passive heat output of heat conduction, natural convection and radiation – so called calm cooling. Correspondingly, the prevailing operating temperature is governed by the complex interaction between operation dependent power losses and passive heat output, as illustrated in **Figure 1**. In order to guarantee a temperature stable process of electrohydraulic compact drives – or vice

versa to know about the possible fields of application – the knowledge of the thermo-energetic properties is essential.

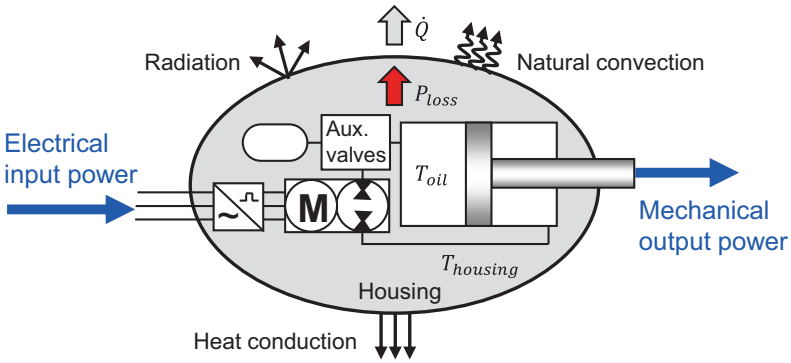

Figure 1: Thermal behaviour of electrohydraulic compact drives /1/

In avoidance of elaborate experiments a lumped parameter simulation is suitable to evaluate the thermo-energetic behaviour of electrohydraulic compact drives. Dynamic and thermo-energetic behaviour with interdependencies as well as dependencies on the operating point can be predicted with reasonable computational effort. The question that has to be answered is, which accuracy in temperature prediction can be achieved and, moreover, is the achieved accuracy satisfying in technical terms. In /1/ an approach was published, how to set up and parameterise a thermo-hydraulic model of an electrohydraulic compact drive demonstrator. First validation results were presented, whereby the accuracy did not match the technical needs yet.

This paper focuses on the prediction of the thermo-energetic behaviour of an electrohydraulic compact drive demonstrator with a thermo-hydraulic model, which was further developed and enables the prediction of operating temperature with sufficient accuracy. Implemented measures to enhance the thermo-hydraulic model are introduced. Additionally, investigation on heat transfer processes on a model shape geometry is presented, which underpins the choice of parameterisation method regarding natural convection. The model is validated against measurements and characteristic results are presented. Apart from thermocouples inside the hydraulic circuit a high-quality thermographic camera is used to provide a detailed capture of outer surface temperatures. Subsequently a further analysis of simulation results is given, highlighting the power losses and heat rejection capabilities of different components. Finally, approaches for the improvement of heat rejection capabilities of the drive are proposed.

2. Electrohydraulic compact drive demonstrator

Before the methodology of thermo-energetic simulation is focused, the electrohydraulic compact drive demonstrator is introduced. A hydraulic scheme and the mechanical design is given in **Figure 2**. Drive's cylinder (1) is controlled by the pump (5), which is driven by a BLDC-motor (6). The differing volume flows of the single rod cylinder are balanced by a hot oil shuttle valve (3), which is connected to a membrane accumulator (4). Adapter- and mounting plates (7, 8) are used to assemble components. The drive is mounted on the cylinder's head side to the test rig (9). More details on the fundamental behaviour of the presented hydraulic circuit can be found in /2/, /3/ and /4/.

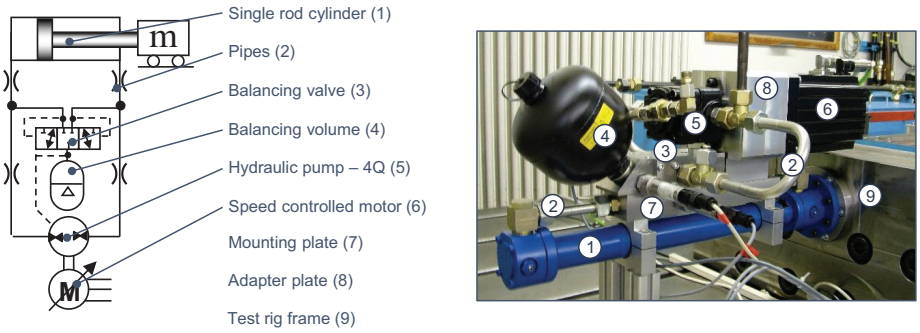

Figure 2: Set-up and design of the electrohydraulic compact drive demonstrator /1/

3. Thermo-energetic modelling of the demonstrator

Thermo-energetic systems simulation with lumped parameters is used in different engineering domains, i.e. in electrical engineering /5/, machine tool engineering /6, 7/ as well as in hydraulic domain /8, 9, 10/. The methodology, which is basically applied, consists of the thermo-energetic analysis and the thermo-energetic modelling and simulation of the system.

The thermo-energetic analysis includes analysis of power losses, which can be regarded as system's heat sources, analysis of heat flows, which represent the paths to the heat sinks and the analysis of thermal resistances located on the way.

Gathered information from thermo-energetic analysis is used to set up and parameterise an energetic and a thermal model that are connected to a dynamic drive model. The resulting thermo-hydraulic model enables the simulation of complex dynamic and thermal processes. In this work, ITI SimulationX®, a commercial multi domain system simulation software, is used as simulation tool.

A detailed description of the thermo-energetic analysis and thermo-energetic modelling of the demonstrator can be found in /1/. In this paper the focus is set on the measures that are taken to further develop the existing thermo-hydraulic model. These are in particular:

- Detailed investigation and implementation of pump efficiency in dependency of operating temperature.
- Basic research on heat transfer at a model shape geometry (cube) regarding natural convection; consequent use of 3D-method to calculate heat transfer number in case of natural convection.
- Refinement of the thermal resistance network.

3.1. Temperature dependent pump efficiency

Main losses in electrohydraulic compact drives are induced by the electric motor and the pump. Subsidiary, friction and flow losses in the cylinder, flow losses in hydraulic piping (including auxiliary valves), accumulator losses as well as frequency converter losses are present. Losses of both motor and pump are dependent on the operating parameters speed and load. Furthermore, in particular pump losses may vary with the operating temperature due to changing fluid viscosity and gap widths /11/. Since temperature dependency was not included in the pump loss model yet, measurements were carried out to quantify temperature influence on efficiency of the used pump. **Figure 3** illustrates the measured pump efficiency in dependency of speed and load at different temperature levels. The results show that with rising temperature the efficiency of the pump decreases especially under high loads, but also increases slightly at higher speeds and small loads.

The complex power loss characteristic of the pump is implemented in form of a 3-dimensional efficiency map $\eta_{Pump} = f(\Delta p, n, \vartheta)$ in simulation – parameterised with the data from measurement. It showed that the implementation of temperature dependent pump efficiency contributes significantly to the enhancement of the accuracy of the thermo-hydraulic model.

Similarly, power losses of the electric motor and friction losses of the cylinder are implemented as 2D-efficiency maps with measured data: $\eta_{Motor} = f(M, n)$, $\eta_{Cylinder} = f(\Delta p, \dot{x})$ respectively. Flow losses are computed by throttle and valve elements.

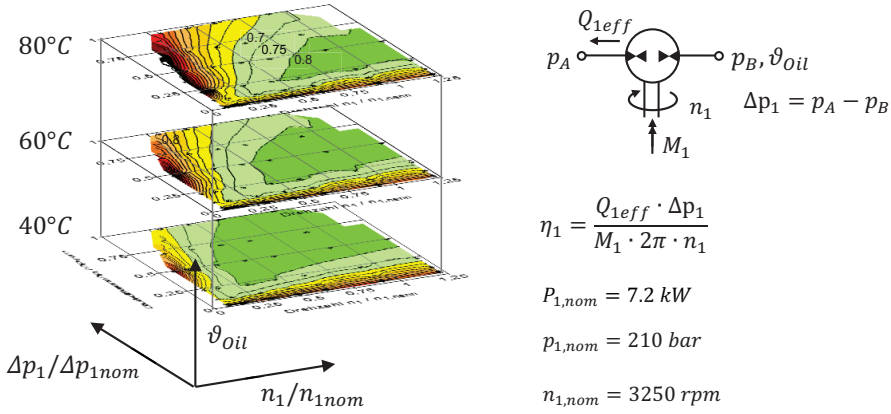

Figure 3: Pump efficiency in dependency of operating temperature

3.2. Calculation of natural convection heat transfer number

The relevant mechanisms on heat transfer on electrohydraulic compact drives are: Enforced convection (inside hydraulic circuit), heat conduction and carriage inside and between solids as well as natural convection and radiation at the free outer surfaces. In case of natural convection the determination of heat transfer numbers is associated with a number of uncertainties. First, the ambient conditions have to be mentioned, which often are not well known. Indoor air flows may influence the heat transfer number in the range of more than 30 % /6/. Second, in literature different approaches exist to calculate natural convection heat transfer problems. Basically the convective heat transfer $\dot{Q}_{con}$ is described by

$$\dot{Q}_{con} = \alpha_{con} \cdot A \cdot \Delta T, \tag{1}$$

with the related area A, the forcing temperature difference ΔT and the heat transfer number

$$\alpha_{con} = Nu \cdot \lambda_{fluid}/L. \tag{2}$$

Here, λ_{fluid} is the heat conductivity of the fluid and L the characteristic length. The Nusselt number Nu, a function of Grashof number Gr and Prandtl number Pr (equation(3)), is calculated for different convection problems by using approaches from relevant tables.

$$Gr = g \cdot L^3 \cdot \beta_{fluid} \cdot \Delta T/\nu^2, Pr = \eta \cdot c_{p,fluid}/\lambda_{fluid} \tag{3}$$

The approaches for calculating Nusselt number either refer to 2D-geometry (horizontal plate, vertical plate), which can be composed to a body, or 3D-geometry as a whole (cube, cylinder and sphere). Both approaches can be found in literature for modelling technical objects, i.e. /6, 7, 9, 10/.

Considering a cube oriented parallel to the ground as simple example, according to /13/ the corresponding approaches for the calculation of Nusselt number are:

$$Nu = 0.766 \cdot [Gr \cdot Pr \cdot f_2(Pr)]^{0,2} \quad \text{Upper horizontal plate}$$

$$Nu = \{0.825 + 0{,}387 \cdot [Gr \cdot Pr \cdot f_1(Pr)]^{1/6}\}^2 \quad \text{Vertical plate} \quad \Big\} \text{2D} \qquad (4)$$

$$Nu = 0.6 \cdot [Gr \cdot Pr \cdot f_1(Pr)]^{0,2} \quad \text{Bottom horizontal plate}$$

$$Nu = 5{,}748 + 0{,}752 \cdot (Gr \cdot Pr / f_4(Pr))^{0,252} \quad \text{Cube} \quad \Big\} \text{3D} \qquad (5)$$

$$f_1(Pr) = \left[1 + (0.492/Pr)^{9/16}\right]^{-16/9}, \; f_2(Pr) = \left[1 + (0.322/Pr)^{11/20}\right]^{-20/11}$$

$$f_4(Pr) = \left[1 + (0.492/Pr)^{9/16}\right]^{16/9}$$

If one applies the two approaches on a given cube geometry, divergences between the calculated convective heat transfers become apparent. In case of entities, which have a homogeneous temperature distribution, it is reasonable to suppose that a 3D-approach matches the convective behaviour better, since the influence of edges and the geometry as a whole is respected. In order to prove this assumption and to test the applicability of the given approaches, a detailed investigation on a cube model shape geometry was carried out.

The used test set-up is illustrated in **Figure 4**. The model geometry is an aluminium cube, which is mounted freely hanging in a self-contained, windowless room. It can be assumed that except self-induced air flows no other air flows are present in this room. The surface of the cube is covered with chalk spray in order to achieve a defined emissivity ε. As heat source a heating cartridge is installed in the centre of the cube, whose heating power is captured by measuring the electric input power. In steady-state the input heating power equals the rejected heat flow. The surface temperature is captured by a thermographic camera.

The diagram in Figure 4 shows the measured temperature of the cube against the convective heat flow. The convective heat flow $\dot{Q}_{con}$ is determined by subtracting the calculated radiative heat flow $\dot{Q}_{rad}$ from the measured input heating power P_{heat}:

$$\dot{Q}_{con} = P_{heat} - \dot{Q}_{rad} = P_{heat} - \varepsilon \cdot \sigma_S \cdot (T^4_{surf,meas} - T^4_{amb,meas}) \quad (6)$$

Further the calculated theoretical values according to equation (1) to (5) are depicted as dashed lines. In comparison 3D-method method fits better the measured values as 2D-method. The average deviation in terms of heat rejection capability is 3.8 %, in contrast to 12.6 % for the 2D-method. Thus, 3D-approach is used consequently for the calculation and parameterisation of natural convection heat transfer processes in the simulation. If the proportion of dimensions is far from one, a decomposition of geometry is done.

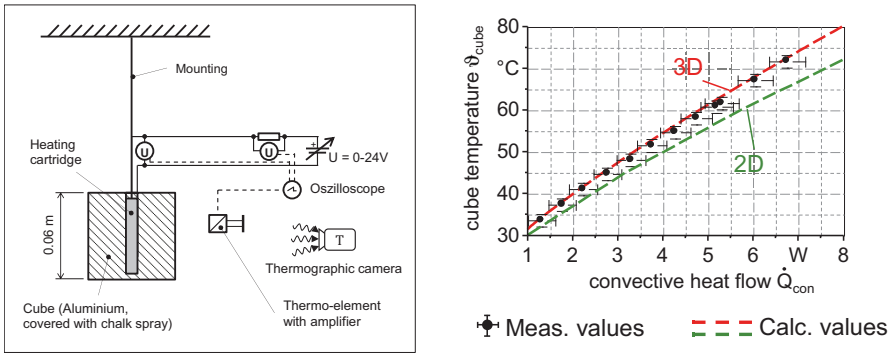

Figure 4: Investigation of natural convection heat transfer processes on a cube

Furthermore, the cube can be used as a reference object to determine ambient conditions, since the heat rejection is well known for ideal, uninfluenced conditions through the investigation. Placing the heated cube next to the compact drive during validation measurements, the test set-up provides information on the influence of occurring indoor airflows and, consequently, strengthens the validation of the model.

3.3. Thermal resistance network

Figure 5 depicts the scheme of the demonstrator's thermal resistance network. With respect to the inclusion of secondary matter components in addition to the main components as well as the consequent use of 3D-method for natural convection processes it is discretised in seven fluidic control volumes A to G and eighteen solid control volumes 1 to 18. The latter represent the housing of the components and the solid construction elements. The heat capacities, which are assigned to each control volume, are connected via thermal resistances to one another, the ambience and the test rig. The thermal resistances R_{th} are determined by the heat transfer number α and the corresponding area A corresponding to the relation

$$R_{th} = 1/(\alpha \cdot A). \quad (7)$$

They consist of enforced convection at the boundaries of the hydraulic system, heat conduction and carriage in the housing and between the demonstrator and the test rig as well as free convection and radiation on the free outer surfaces. The calculation of the heat transfer numbers is done by means of approaches from relevant tables and publications /6, 12, 13/. The losses of the components are inscribed at the control volumes, where they are transferred into the system. Not illustrated in the scheme are the flow losses of the piping.

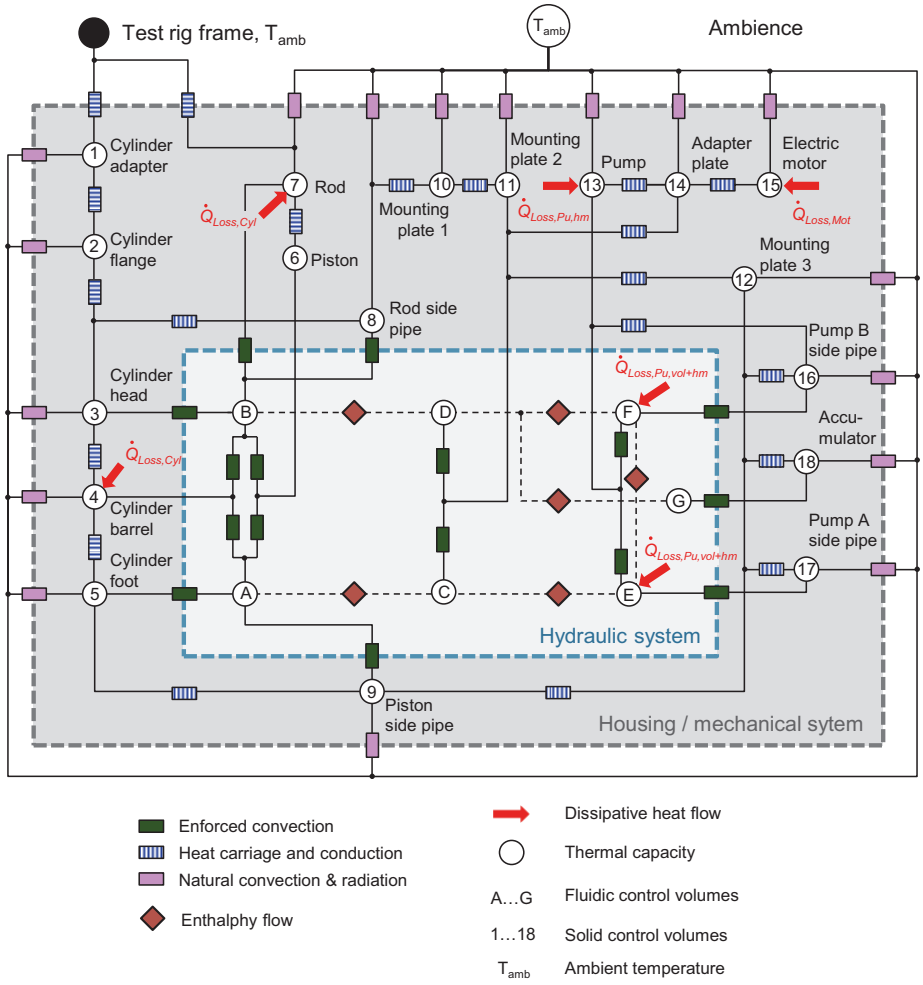

Figure 5: Thermal resistance network of the demonstrator

Basis for the calculation of system's temperatures is the first law of thermodynamics

$$\frac{dE}{dt} = \sum_i \dot{Q}_i(t) + \sum_j P_j(t) + \sum_k \dot{m}_k \left[h + \frac{c^2}{2} + gz\right]_k, \tag{8}$$

which has to be satisfied for each control volume, whereby kinetic and potential energy can be neglected.

4. Test rig and duty cycle

For the validation of the thermo-hydraulic model of the demonstrator the test rig set-up according to **Figure 6** was used. The demonstrator is connected to a moveable mass, on which a desired load force can be applied by means of an electrohydraulic load simulator. Apart from power related quantities the temperature at relevant locations in the system is measured. The oil and the ambient temperature is captured by thermocouples, the outer surface temperatures by a high quality thermographic camera. The thermographic camera provides a detailed capture of outer surface temperatures and enables a validation of surface temperatures in a greater depth.

Additionally, the in chapter 3.2 investigated cube is placed next to the demonstrator. The surface temperature of the heated cube is captured by the thermographic camera as well. The deviation to the thermal behaviour under ideal conditions is a measure for the indoor airflows occurring during the experiment. On the basis of the measured data an averaged correction factor for the convective heat flow is derived, which has the value of 1.16 between the prevailing and the uninfluenced convective heat flow. The correction factor is implemented in simulation and strengthens the validation of the model.

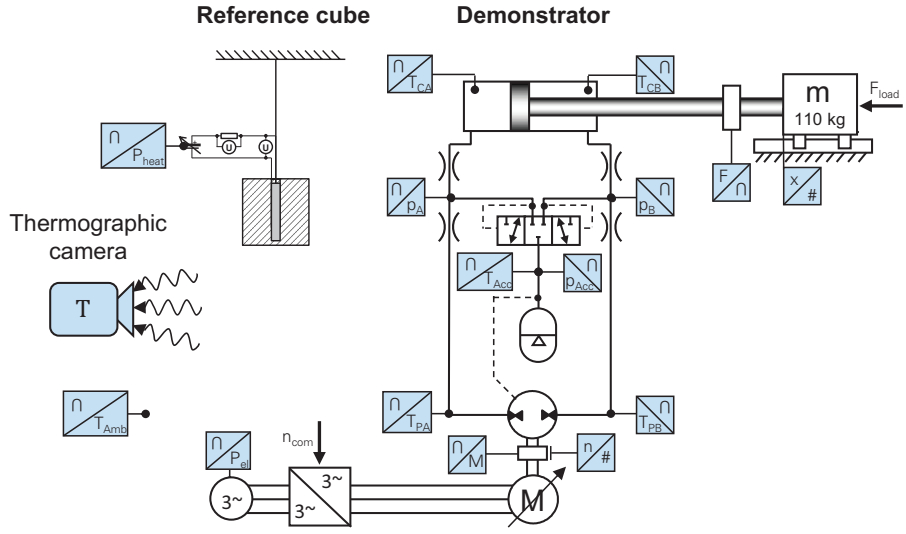

Figure 6: Test rig set-up

As duty cycle, the drive executed a harmonic oscillation of position x with a frequency of $f = 0.4\ Hz$ and an amplitude of $\hat{x} = 120\ mm$. The applied load force was set constantly to $F_{load} = 5\ kN$.

5. Results

5.1. Model validation

Looking at the balance of power a good congruence between simulation and measurement can be stated. The amount of electric energy consumed by the drive executing the prescribed duty cycle differs only to a small extent (about one percent). The simulated and measured oil and surface steady-state temperatures are illustrated in **Figure 7**. It shows that simulated temperatures match measured ones closely with a slight overestimation of oil temperatures. The maximum oil temperature in the system differs 4.4 % between measurement and simulation. Particularly noticeable is the overestimation of oil temperature on the rod side of the cylinder, where the deviation is 15 %. The solid material at the same place (cylinder head) shows the opposite behaviour. This suggests that in the experiment a larger amount of heat is transferred into this component and subsequently to the ambience.

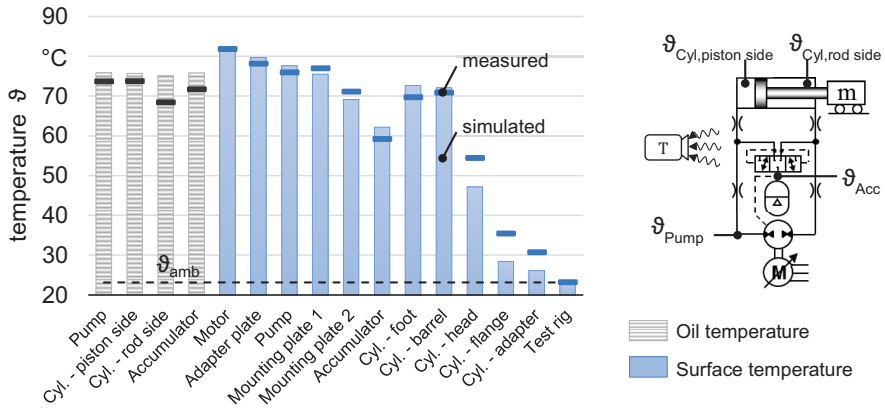

Figure 7: Simulated and measured steady-state temperatures

Even though the thermo-hydraulic model was further developed, various uncertainties in describing thermal and loss behaviour remain. Uncertainties in the parameters, which are necessary to describe the heat carriage between connected surfaces or the reduction to simple model geometries are mentioned exemplarily. Moreover dynamic losses are not taken into account, since steady-state efficiency maps are used to model the loss behaviour of motor, pump and cylinder. In terms of validation the measurement accuracy

of temperature capture has to be mentioned, which is given with ±1.5 K for the thermographic camera and ±0.5 K for the thermocouples.

Nevertheless, even though the simulated temperatures do not perfectly match the measured ones, simulation predicts the thermo-energetic behaviour with satisfying precision in order to support development, optimisation and examination of possible fields of application of electrohydraulic compact drives.

Furthermore, the thermo-hydraulic model can be used to analyse drive's thermal behaviour in depth. The left diagram in **Figure 8** shows the power losses and heat rejection distribution among the components. Clearly, pump and motor are the main heat sources, while the most heat rejecting components are the cylinder and the motor. The right handed diagram illustrates the dominant heat transfer mechanisms. With a total heat rejection of approximately $\dot{Q} = 500\,W$ most heat is transferred by natural convection, followed by radiation and conduction.

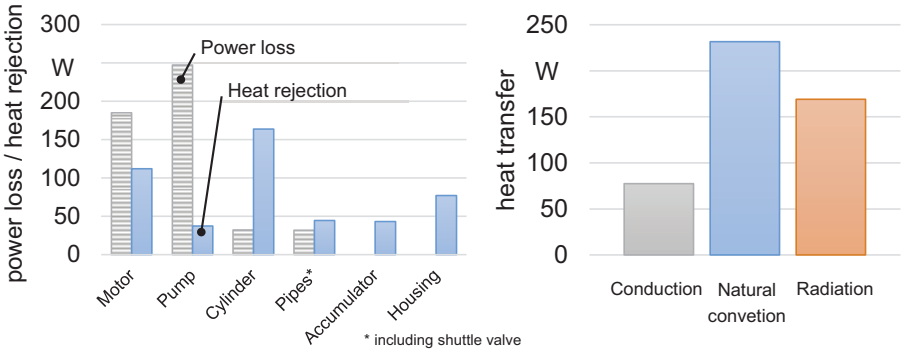

Figure 8: Simulated distribution of steady-state power losses and heat rejection

5.2. Heat rejection improvement studies

Moreover, the validated thermo-hydraulic model enables studies on the heat rejection improvement. Approaches for the improvement of heat rejection are covering blank metallic surfaces with high emissive coatings ($\varepsilon_{metal} = 0.05 \ldots 0.24$, $\varepsilon_{varnish} = 0.92 \ldots 0.97$) or provide ribbed surfaces to increase radiative and convective heat transfer respectively. The calculation of heat transfer numbers of ribbed surfaces can be found in /6/.

Figure 9 shows the simulated temperatures of the demonstrator with improved heat rejection behaviour. All metallic surfaces are varnished ($\varepsilon_{varnish} = 0.92$) and the motor as well as the mounting plates are equipped with ribbed surfaces. With these measures the maximum oil temperature can be reduced by 22 % from 76 to 64°C.

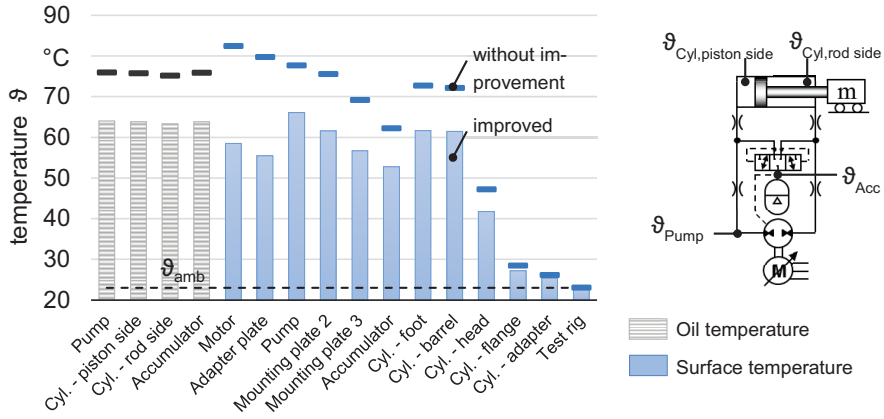

Figure 9: Simulated steady-state temperatures of conventional and improved demonstrator

6. Conclusion

Electrohydraulic compact drives represent an interesting alternative to conventional hydraulic or electromechanical drives. Due to the calm cooling (passive heat output) the prediction of thermo-energetic behaviour is essential in order to guarantee a thermally stable process without elaborate experiments. System simulations with lumped parameters are suitable to predict thermo-energetic behaviour with reasonable computational effort. In this paper, a lumped parameter thermo-hydraulic model of an electrohydraulic compact drive demonstrator is introduced, which combines a dynamic system model with a thermal resistance network. The thermal resistances are parameterised analytically by means of approaches from literature. Further, in particular the temperature dependent losses of the pump and the natural convection heat transfer of a model shape geometry (cube) are focused. Profound studies of the latter enables the identification of ambient conditions during experiments using the cube as a reference object. The validation against measurements shows that the model achieves an accuracy of 4.4 % in the prediction of the system's maximum steady-state oil temperature. This accuracy can be considered as satisfying in technical terms in order to support development, optimisation and examination of possible fields of application of electrohydraulic compact drives. Finally, an analysis of power losses and heat rejection capabilities among the components and a simulation study on the improvement of the heat rejection capability is presented. It is shown that with the use of ribbed surfaces and varnish the system's maximum oil temperature can be reduced by 22 %. Future works will target sensitivity analysis of the thermo-hydraulic model and thermo-energetic behaviour as well as aspects of wear and oil aging in electrohydraulic compact drives.

7. Acknowledgement

Supported by:

on the basis of a decision
by the German Bundestag

The research presented in this paper is based on the project "Thermischer Haushalt und Verschleiß elektrohydraulischer Kompaktantriebe" (Ref.-No. AiF 18051 BR), which is financed and supervised by the Research Association Mechanical Engineering (FKM). In the scope of the Programme to promote Industrial Collective Research it is funded by the German Federation of Industrial Research Associations (AiF) with means of the Federal Ministry of Economic Affairs and Energy (BMWi) on the basis of a decision by the German Bundestag.

8. References

/1/ Michel, S., Schulze, T., Weber, J.: Energy-efficiency and thermo energetic behaviour of electrohydraulic compact drives. 9th International Fluid Power Conference, Aachen, Germany, Vol. 1, pg. 162–177, 2014

/2/ Williamson, C.: Power Management for Multi-Actuator Mobile Machines with Displacement Controlled Hydraulic Actuators. Dissertation, Purdue University, 2010

/3/ Michel, S., Weber, J.: Electrohydraulic Compact Drives for Low Power Applications considering Energy-efficiency and High Inertial Loads. Seventh FPNI-PhD-Symposium, Reggio Emilia, Italy, pg. 869-888, 2012

/4/ Michel, S.; Weber, J.: Energy-efficient electrohydraulic compact drives for low power applications. In: Johnston, D. N. (ed.): Fluid Power and Motion Control (FPMC 2012). Bath, 2012, pg. 93-107

/5/ Nerg, J., Rilla, M., Pyrhönen, J.: Thermal Analysis of Radial-Flux Electrical Machines with a High Power Density. IEEE Transactions on industrial electronics, Vol. 55, No. 10, 2008

/6/ Jungnickel, G., Simulation des thermischen Verhaltens von Werkzeugmaschinen – Modellierung und Parametrierung. Technische Universität Dresden, 2010

/7/ Buchman, K.; Jungnickel, G.: Wärmeübertragung an Be- und Verarbeitungsmaschinen. Wroclaw : Wydawnictwo politechniki wroclawskiej, 1978

/8/ Sidders, J. A.; Tilley, D. G.; Chapple, P. J.: Thermal-hydraulic performance prediction in fluid power systems. Journal of Systems and Control Engineering, Volume 210 (1996), Nr. 49, pg. 231–242, 1996

/9/ Rahmfeld, R.: Development and Control of Energy Saving Hydraulic Servo Drives for Mobile Systems, Dissertation, TU Hamburg-Harburg, 2002

/10/ Busquets, E.; Ivantysynova, M.: Temperature Prediction of Displacement Controlled Multi-Acutator Machines. International Journal of Fluid Power, Vol. 14, No. 1, pg. 25-36, 2013

/11/ Ivantysyn, J.; Ivantysynova, M.: Hydrostatische Pumpen und Motoren : Konstruktion und Berechnung. Würzburg : Vogel, 1993

/12/ Yovanovich, M. M.; Thermal contact correlations. In: AIAA 16th Thermophysics Conference, Palo Alto, June 23-25, 1981. New York : AIAA, 1981, pg. 83-95

/13/ Verein deutscher Ingenieure - VDI-Gesellschaft Verfahrenstechnik und Chemieingenieurwesen (GVC) (Publ.): VDI-Wärmeatlas, Springer, 2013.

9. Nomenclature

A	Area	m^2	Q	Volume flow	l/min
c	Flow velocity	m/s	$\dot{Q}$	Heat flow	W
c_p	Specific heat capacity	J/(kg*K)	p	Pressure	N/m²
E	Energy	J	P	Power	W
f	Frequency	Hz	Pr	Prandtl number	-
F	Force	N	R_{th}	Thermal resistance	K/W
g	Gravity	m/s^2	t	Time	s
h	Specific enthalpy	J/kg	T	Temperature	K
Gr	Grashof number	-	U	Voltage	V
L	Characteristic length	m	x	Position	m
$\dot{m}$	Mass flow	kg/s	z	Height	m
M	Torque	Nm	α	Heat transfer number	W/(m²*K)
n	Speed	rev/min	β	Expansion coefficient	1/K
Nu	Nusselt number	-	ε	Emissivity	-

η	Efficiency, Dynamic viscosity	-, kg/(m*s)
λ	Heat conductivity	W/(m*K)
ν	Kinematic viscosity	m^2/s
σ_S	Boltzmann constant	J/K
ϑ	Temperature	°C